Universidad Tecnológica Nacional
DICIEMBRE 2020 / Año 18- Nº 39

Revista Tecnología y Ciencia
DOI: https://doi.org/10.33414/rtyc.39.41-61.2020 - ISSN 1666-6933

Microencapsulation of Grapefruit Oil with Sodium Alginate by Gelation and Ionic Extrusion: Optimization and Modeling of Crosslinking and Study of Controlled Release Kinetics.

Microencapsulación de aceite de pomelo con alginato de sodio por gelificación y extrusión iónica: optimización y modelado de la reticulación y estudio de la cinética de liberación controlada.

Presentación: 16/07/2020

Aprobación: 03/09/2020

Liliana M. Cáceres
Centro de Investigación en Química Orgánica Biológica, Facultad Regional Resistencia (FRRe), Universidad Tecnológica Nacional (UTN) - Instituto de Modelado e Innovación Tecnológica, Consejo Nacional de Investigaciones Científicas y Técnicas (CONICET), Universidad Nacional del Nordeste (UNNE). Resistencia, Chaco – Argentina
lmarielc@yahoo.com.ar

Gustavo A. Velasco
Centro de Investigación en Química Orgánica Biológica, Facultad Regional Resistencia (FRRe), Universidad Tecnológica Nacional (UTN) - Instituto de Modelado e Innovación Tecnológica, Consejo Nacional de Investigaciones Científicas y Técnicas (CONICET), Universidad Nacional del Nordeste (UNNE). Resistencia, Chaco – Argentina
gavelasco@arnet.com.ar

Eliana P. Dagnino
Centro de Investigación en Química Orgánica Biológica, Facultad Regional Resistencia (FRRe), Universidad Tecnológica Nacional (UTN) - Instituto de Modelado e Innovación Tecnológica, Consejo Nacional de Investigaciones Científicas y Técnicas (CONICET), Universidad Nacional del Nordeste (UNNE). Resistencia, Chaco – Argentina
epdagnino@gmail.com

Ester R. Chamorro
Centro de Investigación en Química Orgánica Biológica, Facultad Regional Resistencia (FRRe), Universidad Tecnológica Nacional (UTN) - Instituto de Modelado e Innovación Tecnológica, Consejo Nacional de Investigaciones Científicas y Técnicas (CONICET), Universidad Nacional del Nordeste (UNNE). Resistencia, Chaco – Argentina
mandhy@hotmail.com

Revista Tecnología y Ciencia
DOI:https://doi.org/10.33414/rtyc.39.41-61.2020 - ISSN 1666-6933

Abstract

Essential grapefruit oil with high concentrations of limonene is used in food, cosmetic and pharmaceutical industries due to its antimicrobial properties, fragrance, and flavour. To facilitate its manipulation and protect it from adverse environmental factors, the microencapsulation is used. The objective of this work was to optimize the microencapsulation process of grapefruit essential oil using external ionic gelation coupled to extrusion with sodium alginate and calcium chloride. We achieved the best encapsulation conditions with calcium chloride concentration at 7.4% w/v and a crosslinking time of 58 minutes, obtaining a yield of 62% and an efficiency of 100% with an oil loading capacity of 10% w/w. The chemical adsorption of calcium as well during the crosslinking process was studied, observing a significant fit with the Elovich equation. And an adjustment of the controlled release of the essential oil was obtained to the empirical kinetic model of Korsmeyer and Peppas.

Keywords: sodium alginate, encapsulation, essential oils, ionic gelation, crosslinking.

Resumen

El aceite esencial de pomelo con alto conteniendo de limoneno tiene aplicaciones en la industria alimenticia, cosmética y farmacéutica debido a sus propiedades antimicrobianas, su aroma y sabor. Para facilitar su manipulación y protegerlo de los agentes ambientales externos se lo microencapsula. El objetivo de este trabajo fue optimizar el proceso de microencapsulación del aceite esencial de pomelo utilizando gelificación iónica externa acoplada a extrusión con alginato de sodio y cloruro de calcio. Los mejores resultados de encapsulación se obtuvieron con una concentración de cloruro de calcio de 7,4% p / v y un tiempo de reticulación de 58 minutos, obteniendo un rendimiento del 62% y una eficiencia del 100% con una capacidad de carga de aceite del 10% p / p. Se estudió la adsorción química de calcio en el proceso de reticulación observando un ajuste significativo con la ecuación de Elovich, y se obtuvo el ajuste de la liberación controlada del aceite esencial con el modelo cinético empírico de Korsmeyer y Peppas.

Palabras claves: alginato de sodio, encapsulación, aceite esencial, gelación iónica, reticulación.

Introduction

Grapefruit oil is an essential oil (EO) known as a sub product of the citrus industry, of great interest for its antimicrobial properties. It is a growth inhibitor of Escherichia coli, Staphylococcus aureus, Lactococcus lactis subsp. lactis, Lactococcus lactis subsp. diacetylactis, Leuconostoc mesenteroides subsp. dextranicum and Lactobacillus plantarum (Vasek, et al., 2015; Ribeiro Santos et al., 2017), making it appropriate for the food and pharmaceutical industry.

Furthermore, this type of oil contains a high percentage of limonene (higher than 70%), which makes it attractive for the cosmetic and cleaning industries, and also applicable as a food additive and industrial solvent as well (Bakkali, et al., 2008). Citrus essential oils represent 0.27% of the total export from Argentina, so it could be considered as a product with great potential for industrial development (Federcitrus, 2018).

Industrial applications of EO are limited by their high degree of volatility, a characteristic that significantly affects the yield of these processes (Soliman et al., 2013). Furthermore, their sensibility to external agents like ultraviolet light, high temperatures, and water, may

Revista Tecnología y Ciencia
DOI:https://doi.org/10.33414/rtyc.39.41-61.2020 ISSN 1666-6933

affect their composition, which facilitates the loss of some specific properties (Lv et al., 2012). As a matter of fact, it is necessary to develop a system that may protect them and facilitate their manipulation (Chen et al., 2017; Kuang et al., 2010).

Microencapsulation is a coating technique which may be used as a system of protection of the agent or coating component, to protect them from external factors. In the case of EO, it also allows small dosages (Benavidez, Cortés, Parada and Franco, 2016; Aghbashlo et al., 2012).

In recent years, there has been a growing interest in microencapsulation of EO with biodegradable materials. Applications were reported in the pharmaceutical industry (Balanc et al., 2016; Goh et al., 2012; Liakos et al., 2014; Liu et al., 2012), in the nutraceutical industry (Mokhtari et al., 2017) and in the food industry (Arriola et al., 2019; Laokuldilok et al., 2016; Lupo et al., 2015) for the immobilization of enzymes or bacteria in bioprocesses. (Ding and Shah, 2007; Shory, 2017; Aguiar et al., 2016).

Several methods of EO microencapsulation have been described for different authors, such as spray drying (Baranauskiene et al., 2006; Aghbasho et al., 2012; Tuyen et al., 2014), coacervation (Dima et al., 2014; Jun-Xia et al., 2011) and ionic gelation (Chan et al., 2000; Liakos et al., 2014; Hosseini et al., 2013).

Ionic gelation by extrusion is an encapsulation technique which presents great adaptability to different types of active principles, whether hydrophobes or hydrophilics, and is a low-cost procedure (Arriola et al., 2019).

Optimization of EO microencapsulation with alginate has been currently studied for its implementation in the food industry considering its antimicrobial properties, smell and taste (Noppakundilograt et al., 2015; Soliman et al., 2013; Goitia Funes and Amurrio Derpic, 2016). Furthermore, sodium alginate is one of the polymeric materials widely used as a matrix to encapsulate active principles due to its biocompatibility, biodegradability and inherent nature (Hosseini et al., 2013; Chuah et al., 2009). It is composed of β-D-mannuronate and α-L-guluronate units linked by 1-4 β-(1–4) guluronic acid units (Liakos et al., 2014; Levic et al., 2016). The alginate has the capacity of producing ionically cross-linked hydrogels, known as the "egg-box model" and generally accepted as the gelation mechanism (Lertsutthiwong et al., 2008). The crosslinking mechanism involves an intermolecular union between divalent cations (for example, calcium) and carboxyl groups in the residues of the guluronic acid of linear polymer chains (Belscak-Cvitanovic et al., 2016). The concentration of calcium chloride solution and the crosslinking reaction have an effect on the efficiency and yield during the encapsulation process. The matrix obtained after crosslinking can lead to a controlled release (Bal et al., 2013) with a release mechanism of the active components sustained in time (Finch, 2005).

In this study, we optimized the microencapsulation process of the grapefruit essential oil, a regional product with a high percentage of limonene, through external ionic gelation with sodium alginate by extrusion. We applied a two-factor experimental design with three levels in order to obtain a high concentration of EO. The concentration of calcium chloride and the crosslinking time were analyzed in terms of yield and efficiency of microencapsulation. We analyzed the controlled release as well, and the characteristics of the microcapsules.

Material and Methods

Material

It was employed a sodium alginate solution (Aldrich with 39% L-guluronic acid and 61% of mannuronic acid, molecular weight of 120,000-190,000 g/mol) and anhydrous calcium

Revista Tecnología y Ciencia
DOI:https://doi.org/10.33414/rtyc.39.41-61.2020 - ISSN 1666-6933

chloride (Cicarelli). Grapefruit essential oil was provided by Mager Enterprise (from the province of Corrientes, in the northeast of Argentina).

Chemical constitution of grapefruit essential oil

Identification of grapefruit EO components were conducted by gas chromatography-mass spectrometry (GC/MS). A two-capillary column QP 5050 Shimadzu equipment was used: one SE 52 (Mega, Legnano, Italia) chemically bonded (25 m x 0.25 mm internal diameter; 0.25 µm thick stationary phase) column, covered by 5% phenil-polydimethylsiloxane (0.25 µm thick stationary phase) at a column temperature of 60 °C (8 min), increasing up to 180 °C at a 3 °C/min speed, then up to 230 °C at a 20 °C/min speed. 250 °C injector temperature, split injection mode; 1:40 split ratio; 0.2 µl oil injection volume. Mobile phase: Helium, 122.2k Pa (51.6 cm/sec), 250 °C interface temperature and 40-400 m/z mass range acquisition. Another BP-20 (SGE, Australia) 25 m x 0.25 mm internal diameter fused silica capillary column covered by polyethyleneglycol 20.000 Da (0.25 µm thick stationary phase). Column temperature at 40 °C (8 min), increasing up to 180 °C (3 °C/min), and up to 230 °C (20 °C/min). 250 °C, injector temperature, split injection mode; 1:40 split ratio; 0.2 µl oil injection volume. Mobile phase: Helium, 92.6 kPa (55.9 cm/s), 250 °C interface temperature and mass range acquisition: 40-400 m/z. Fragmentation patterns in each component were compared to those stored in the software library spectra (Mc Lafferty and Stauffer, 1991; Adams, 2001).

Preparation of solutions and alginate-oil emulsion

A calcium alginate solution was dissolved in deionized water (0.2 µS conductivity, 40 °C) at a concentration of 1% w/v by soft mechanical stirring. Then, the resulting solution was left standing for an hour in order to de-gas it. After that, the viscosity of the alginate solution was sized with a Ni-Run NDJ-8S digital viscometer using a spindle N° 0. The crosslinking solutions were then prepared with anhydrous calcium chloride in deionized water to 2, 5 and 10% w/v. Separately, 30 g of alginate solution was mixed with the specific amount of grapefruit oil necessary to obtain a 10% w/v load. The DLAB D500 homogenizer used was at 2000 rpm for three minutes to obtain a homogeneous distribution of the emulsion. To assure its stability, the solution was then left standing for an hour, observing if the separation of phases took place (Chan, 2011; Levic et al., 2015).

Microscopic observation

The degree of dispersion and homogeneity of the emulsion was determined by measuring the droplet size and calculating the polydispersibility (Mabille et al., 2000). These statements were applied following the Benavides et al. methodology (2016) with slight modifications. Degasification was then performed by putting the emulsion into an ultrasonic bath with a frequency of 40 khz (Digital Utrasonic Leaner, ARCANO) with water at room temperature (25 °C) for three minutes.

After that, the emulsion was observed with a trinocular microscope Lancet SME F6E equipped with a camera (Touptek UCMOS 01300 KPA, TP601300A model, origin China) and data acquisition system (Toup View: Touptek Photonics of Toupteck Corporation) to size the diameter of the droplets. The polydispersibility of the emulsion was calculated with the following equation (1) (Camino, Sánchez, Patino and Pilosof, 2012):

Revista Tecnología y Ciencia
DOI:https://doi.org/10.33414/rtyc.39.41-61.2020 ISSN 1666-6933

$$P = \left(\frac{1}{\overline{d}}\right)\left(\frac{\Sigma\left(d_i^3 x\left|\overline{d} - di\right|\right)}{\Sigma d_i^3}\right) \quad (1)$$

Where di is the droplet diameter and $\overline{d}$ is the average droplet diameter of the emulsion.

Statistical analysis: Optimization of the encapsulation process

Experiments were conducted following a 3^k central composite factorial design, with k=2, and analyzed according to the response surface methodology to estimate the polynomial quadratic equations of optimization (Kuehl, 2000). Calcium chloride (2, 5 and 10% w/v) and time (30, 45 and 60 minutes) were the factors selected, expecting that both were linked to the yield and efficiency in the obtention of microcapsules. All experiments were performed with a 10% w/w load of essential grapefruit oil and with a sodium alginate polymeric solution to 1% w/v. Two replicates of the design were carried out with nine runs each, fulfilling a total of 18 runs. The statistical analysis was performed with Minitab Statistical Software 18.1 (2017), trial. For this specific design, it was employed the following quadratic model (2):

$$y = \beta_0 + \beta_1 x_1 + \beta_2 x_2 + \beta_{12} x_1 x_2 + \beta_{11} x_1^2 + \beta_{22} x_2^2 + \varepsilon \quad (2)$$

Where y is the factor, β_0 is the constant, βi are the mean linear coefficients, β_{ii} are the mean square coefficients, β_{ij} are the mean effect of interactions, x_1 and x_2 are the independent variables, and ε is the random error (Montgomery, 2003). Analysis of Variance (ANOVA) was then performed with a level of statistical significance of 95% ($p<0.05$). In addition, the regression coefficient (R^2), the p-value, the F-value (Fisher Test) and the lack of adjustment were evaluated in order to determine the adjustment of the model. The two responses (yield and efficiency) were maximized. After that, the model was validated with five runs at the optimal point.

Obtention of microcapsules

Microcapsules were obtained following the methodology described by other authors with slight modifications (Chan, 2011; Benavidez et al., 2016). A syringe pump Apema PC11UBT was used to perform extrusion with a needle of internal diameter of 0.21 mm. For this part of the experiment, 10 ml of the emulsion previously prepared were taken with a syringe that was connected in the pump programmed at a dripping speed of 90 mL/h and fixed 5 cm above the surface of the solution. Afterwards, the drops fell into a calcium chloride solution which was prepared according to the design. The gelling solution was gently stirred with a magnetic stirrer over 30, 45 and 60 minutes. The obtained microcapsules were separated from crosslinking with a steel filter net and rinsed into tert-butyl alcohol in order to eliminate oil residues from the surface. Then, the microcapsules were weighed in a balance analyzer and stored in a caramel recipient at 4 °C.

Yield of the encapsulation process

The yield is the rate between the number of microcapsules obtained and the amount of the emulsion used during the encapsulation process. The percentage yield was calculated with the following equation (3) (González et al., 2005):

Revista Tecnología y Ciencia
DOI:https://doi.org/10.33414/rtyc.39.41-61.2020 - ISSN 1666-6933

$$R\% = \frac{w_m}{w_a + w_p} 100 \quad (3)$$

Where w_m is the weight of the filtered microcapsules, w_p is the weight of the polymer solution (sodium alginate) and w_a is the amount of the active components added in order to prepare the emulsion.

Efficiency of the microencapsulation process

The efficiency of the microencapsulation process measures the amount of active components that were encapsulated into the microcapsule.

The calculation was based on the determination by gas chromatography of the microencapsulated limonene mass (Solomon et al., 2012) using the method of internal standards. In order to measure with a chromatography, the microcapsules were filtered with a steel sieve and rinsed with a considerable known amount of tert-butyl alcohol to remove the residual oil from the surface of the microcapsule. A sample of 30 µL of this solution was taken and then 10 µL of methyl isobutyl ketone were added as internal standard. This mixture was analyzed with a Shimadzu GC–14B gas chromatography, Megabore DB-WAX P/N 125-7032 polar column of 30 m long x 0.53 mm of internal diameter x 1 µ thickness, connected to a Flame Ionization Detector (FID). The FID temperature was of 220 °C and for the injector temperature was of 180 °C. The temperature of the column remained isothermal in 40 °C for over two minutes. Then, it increased to 5 °C/min until reaching 180 °C. Lastly, the temperature remained isothermal in 180 °C for over two minutes. The related areas of the chromatogram in a standard curve were compared in order to determine the limonene mass present on the surface (w_s). Afterwards, the weight of the encapsulated limonene was calculated in a specific mass of microcapsules (w_1) stating a difference between the weight of the initial (w_2) and the superficial (w_s) limonene. For this study, the efficiency value was determined as follows (4) (Maji, Baruah, Dube and Hussain, 2007):

$$E\% = \frac{w_1}{w_2} 100 \quad (4)$$

Loss of water during the yield process

The moisture of the microcapsules was determined to evaluate the amount of loss of water during the crosslinking process. Almost 0.8 g of filtered microcapsules were weighed and then placed onto an aluminum tray. In order to determine their moisture, it was employed a Radwag PMR 50 moisture balance analyzer and the measurements were assayed in quintuplicate. The microcapsules used were prepared without oil, with 1% w/v alginate crosslinking in calcium chloride solution to 2, 5 and 10% w/v during the crosslinking time of 30, 45 and 60 minutes.

Morphology of the alginate microcapsules

Microcapsules were observed through an optical microscope equipped with a digital camera in order to measure the sphere diameter. The morphology of the microcapsules was evaluated with a Scanning Electron Microscope (SEM) Jeol 5800 LV. Microcapsules were

Revista Tecnología y Ciencia
DOI:https://doi.org/10.33414/rtyc.39.41-61.2020 ISSN 1666-6933

then placed over the stage and sputtered with a thin coat of gold. Observations were made with different increments at room temperature.

Crosslinking calcium adsorption

After the optimization of the process of obtaining microcapsules, the kinetic yield with the optimized values of calcium chloride concentration and the crosslinking time were studied. Then, 1% w/v of alginate solution in deionized water was placed into the syringe pump, without essential oil, and it dripped on the crosslinking solution of calcium chloride 5% w/v. They were cross-linked during 1, 2, 3, 5, 15 and 30 minutes. Microcapsules were then filtered and rinsed in deionized water. Approximately 30 g of microcapsules were weighed and placed into a crystallizer to get dry. After that, they were placed in an oven at 100 °C for over 12 hours. The dried particles were then transferred to a clean and dried crucible and introduced in a muffle furnace at 750 °C for over eight hours or until they turned to ashes. After that process, dried calcium ions were valued by emission spectrophotometry using Jenway PFP07 flame photometer (Industrial Version). The data obtained was precisely revised in order to discover kinetic adsorption. To obtain this, we employed the Elovich model about the application of general processes of chemisorption, using the following equation (5) (Pinzón-Bedoya and Vera Villamizar, 2009):

$$\frac{dq_t}{dt} = ae^{-bq_t} \tag{5}$$

Where, q_t is the adsorbed amount in time t (mmol/g), a is the initial speed of adsorption (mol/gmin) and b is related to the covered surface and the energy of activation by chemisorption (mmol/g).

Study of the controlled release

The controlled release was performed by placing 8 g of microcapsules obtained during the optimized process in a 50 mL Erlenmeyer with 20 g of tert-butyl alcohol at room temperature with continuous stirring on an orbital shaker. Aliquots of 30 µL were extracted from the solution at regular intervals of 30 minutes until eight hours of release. Then, a diary sample was taken for two days, and after that, a weekly sample was taken until two weeks were completed. The samples were analysed in a gas chromatograph following the exact conditions described above. The experimental data were presented to make the mathematical model after that.

Kinetics analysis of drug release

The mechanism of essential oil release was studied from the matrix to the exterior fitting the data obtained to the semi-empirical model presented as follows (6) (Korsmeyer and Peppas, 1981):

$$\frac{M_t}{M_\infty} = kt^n \tag{6}$$

Where M_t / M_∞ is the fractional solute release, t is the release time, k is a constant characteristic of the macromolecular network system and the substance encapsulated, and n is the diffusional exponent characteristic of the release mechanism.

Revista Tecnología y Ciencia
DOI:https://doi.org/10.33414/rtyc.39.41-61.2020 - ISSN 1666-6933

Results and discussion

Chemical constitution of essential oil

21 components were identified by GC/MS analysis: 9 terpenes, 3 sesquiterpenes, 2 aldehydes, 7 alcohols, and 1 ester (representing 99.10% of the components). The compound present in the highest proportion was limonene (92.6%) near the upper limit of the reported range (76.00-96.00%) for citrus essential oils (Kirbaslar, et al., 2006; Espina, et al., 2011). The complete characterization of the grapefruit essential oil used in this work was carried out in previous studies and published by the authors (Vasek, et al., 2015).

Preparation of solutions and alginate-oil emulsion

The viscosity of the alginate solution at 1% used in the emulsion at 20 °C with a rotor speed of 0.6 rpm was 0.35 kg/ms. This concentration of alginate was established in preliminary studies being ideal for extrusion due to the size of the needle selected. The emulsion prepared with the alginate solution and 10% w/w of grapefruit oil showed stability after an hour of standing, with no phase separation. Levic et al. (2015) reached similar results with grapefruit oil concentrations of 5 and 10% w/v. Chan (2011) demonstrated stability during the same time with oil concentrations from 5 to 40% v/v. Oil drops in the emulsion, observed in the microscope, have an average diameter of 0.0018 mm (Figure 1a), slightly smaller than the diameters obtained by Noppakundilograt et al. (2015) with similar concentrations of alginate emulsion and eucalyptus oil. The polydispersibility calculated with the equation (1) was 0.8, and this value (> 0.5) indicated that it was an emulsion with a broad distribution of diameters. Benavidez et al. (2016) obtained similar polydispersibility values but with lower homogenization speed and less oil concentration, and with a larger average diameter. Additionally, the asymmetry of the sample was calculated and showed a value of 0.36 indicating a positive asymmetry. Thus, it cannot be statistically represented by the sample mean. The mode of the distribution was then calculated, which showed a value of 0.0008 mm. This not-gaussian distribution responded to other distribution models (Sis et al., 2005) and it was a feature of the emulsions prepared at high speeds and with small droplet sizes.

Obtaining of microcapsules

It was possible to obtain spherical microcapsules with a uniform size (Figure 1b) using a dropping distance of 0.05 m and a dropping speed of 90 mL/h (established in preliminary studies).

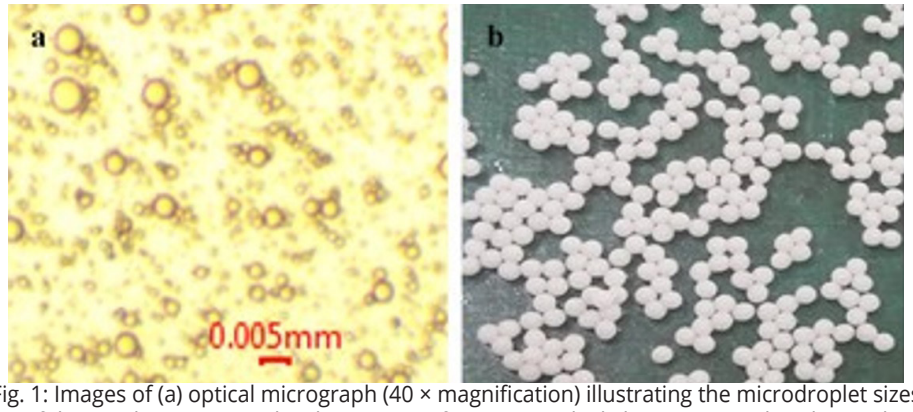

Fig. 1: Images of (a) optical micrograph (40 × magnification) illustrating the microdroplet sizes of the emulsion prepared with 10% grapefruit essential oil, (b) microcapsules obtained

Revista Tecnología y Ciencia
DOI:https://doi.org/10.33414/rtyc.39.41-61.2020 ISSN 1666-6933

Microencapsulation yield and efficiency

The levels of the factors and the percentage results of efficiency and yield reached are illustrated in Table 1. The average yields obtained were set between 42% and 68%. These low yield values stemmed from the loss of water during the crosslinking process, which was demonstrated with the moisture analysis of particles after filtration, as it is shown later on Benavides et al. (2016) achieved a maximum yield of 62% using calcium chloride at 1.5% with loading capacity of oil of 1–3% v/v. Other authors (Ribeiro et al., 1999) obtained yields of 60–80% using double emulsions of oil and water, besides incorporating another wall material such as chitosan. In other studies, they obtained yields from 83.4% to 87.97% encapsulating Zanthoxylum limonella essential oil by multiple emulsion solvent evaporation technique.

As it is shown in Table 1, the efficiency of the microencapsulation was related to time. Maximum efficiency was seen at 60 minutes of crosslinking, reaching an average of 99.86% of efficiency in encapsulation. This value could be related to a longer crosslinking time resulting in a wall with a higher level of rigidity, which reduces the retention of essential oil on the surface during gelation. Another study showed lower efficiency (88.6%) at 60 minutes on the encapsulation of eucalyptus essential oil (Noppakundilograt et al., 2015), and observed also dependence with the crosslinking time and independence with the calcium chloride concentration. Soliman et al. (2013) encapsulated cinnamon oil, clove oil, and thyme oil, and found similar efficiency values in encapsulation (between 90 and 95%) using calcium chloride concentrations of 0.5% and crosslinking times of 20 minutes. Efficiencies found by Hosseini et al. (2013) when encapsulating Satureja hortensis essential oil were lower (from 52.4 to 66.37%) as they used essential oil concentrations below 5%, multiple emulsions, and emulsifying agents.

Experimental runs	Concentration Cl2Ca (% p/p)	Time (min)	Efficiency (% ± S)	Yield (% ± S)
1	2 (-1)	30 (-1)	95.63±2.63	59.06±1.93
2	2 (-1)	45 (0)	94.47±0.67	46.43±5.05
3	2 (-1)	60 (+1)	100.00±0.00	42.42±0.67
4	5 (0)	30 (-1)	95.44±1.66	68.20±3.42
5	5 (0)	45 (0)	98.59±0.11	68.18±0.79
6	5 (0)	60 (+1)	99.58±0.59	52.74±1.88
7	10 (+1)	30 (-1)	95.14±1.62	48.55±6.77
8	10 (+1)	45 (0)	95.29±1.09	53.04±6.31
9	10 (+1)	60 (+1)	100.00±0.00	59.61±2.29

Note. Efficiency and yield: mean% ± mean standard deviation, results of four measurements in each case.

Table 1: Levels of experimental design and results of encapsulation yield and efficiency

Optimization of the microencapsulation process

Efficiency and yield were maximized by the optimization of the process of obtaining grapefruit essential oil microcapsules. In the present study, it was applied the response surface methodology to a second-order 3^k factorial design with two replications. A total of 36 runs

Revista Tecnología y Ciencia
DOI:https://doi.org/10.33414/rtyc.39.41-61.2020 - ISSN 1666-6933

were performed. The statistical analysis showed that the models for encapsulation efficiency and yield were appropriate (Table 2), with a significant R2 (0.85 and 0.83 respectively) and with a p-value of lack of fit larger than 0.05 (α-value) in both cases. The time variable had a significant linear effect (with a p-value smaller than 0.05) on both dependent variables (yield and efficiency). While the calcium chloride concentration did not have a significant linearly influence in any of them (p-value larger than 0.05), it influenced in a quadratic way on the encapsulation yield. Additionally, the quadratic effects were relevant to efficiency. Furthermore, the factors did not have significant interactions in the encapsulation efficiency, so this term could be removed from the mathematical model. However, it is possible that some kind of interaction between these factors existed in the case of the yield.

Factor	Encapsulation Efficiency					Encapsulation Yield				
Source	Sum of squares	d.f.	Mean square	F value	P value	Sum of squares	d.f.	Mean square	F value	p value
Model	85.57	5	17.11	19.03	0.000024	1071.12	5	214.224	11.78	0.000272
Linear	64.73	2	32.33	35.99	0.000008	135.59	2	67.795	3.73	0.055037
A	0.888	1	0.89	0.99	0.339798	35.82	1	35.824	1.97	0.185775
B	63.84	1	63.84	70.99	0.000002	99.77	1	99.765	5.49	0.037226
Quadratic	19.97	2	9.98	11.1	0.001866	479.98	2	239.988	13.2	0.000932
AA	4.81	1	4.82	5.35	0.039205	473.33	1	473.329	26.03	0.000261
BB	15.15	1	15.15	16.85	0.001460	6.65	1	6.648	0.37	0.556673
Interaction	0.13	1	0.13	0.14	0.713368	435.16	1	435.159	23.93	0.000371
AB	0.13	1	0.13	0.14	0.713368	435.16	1	435.159	23.93	0.000371
Residual	10.79	12	0.9			218.2	12	18.183		
Lack of fit	4.89	3	1.63	2.49	0.126413	105.51	3	35.171	2.81	0.100277
Pure error	5.9	9	0.66			112.69	9	12.521		
Corrected total	96.36	17				1289.32	17			
Correlation coefficient (R^2)	0.852					0.830				
Adjusted R2	0.79					0.76				

Note. A: $CaCl_2$ concentration and B: crosslinking time (Independent variables). d.f.: Degree of freedom.

Table 2: Analysis of variance for encapsulation: efficiency and yield

The parameters with the significant coefficients of the efficiency (EE) and yield (R) encapsulation models obtained through the method of least squares are shown in the regression equations (7) and (8), both in uncoded units.

$$EE\% = 103.88 + 0.95A - 0.62B - 0.07AA + 0.01BB \quad (7)$$

Revista Tecnología y Ciencia
DOI:https://doi.org/10.33414/rtyc.39.41-61.2020 ISSN 1666-6933

$$R\% = 65.60 + 3.75A - 0.41B - 0.07AA - 0.01BB + 0.12AB \quad (8)$$

Based on these models, were created the response surface graphics (Figures 2 a-d) to understand the correlation between the results and the levels of each factor (calcium chloride concentration and crosslinking time). As shown in Figure 2a, higher efficiency values were obtained with times of 60 minutes and any value of calcium chloride concentration, whereas the higher yield zone had calcium chloride concentrations between 3 and 7.5% w/v (Figure 2b). The 3D response surface showed the surface curvature according to the second-order model. Figure 2c shows that at times of 60 minutes, there were obtained efficiencies between 99 and 100%, meaning that it was an optimal value of the crosslinking time. Figure 2d shows an optimal curvature point in less than 60 minutes.

The optimization of both variables through the desirability function is shown in Figure 3. The compound desirability (0.84) was good, which means that the combined values of the variables allowed efficiency and yield maximization. However, the individual desirability indicated that the configuration was more effective to maximize efficiency (d=1) than the yield (d=0.71). According to this model, with a calcium chloride concentration of 7.4% w/v and a crosslinking time of 58 minutes, it would be possible to reach a yield of 62% and efficiency of 100% of the encapsulation process. The prediction interval obtained for the yield was 57.62% to 72.86% and for the efficiency of 97.83% to 102.25%, with a confidence level of 95%.

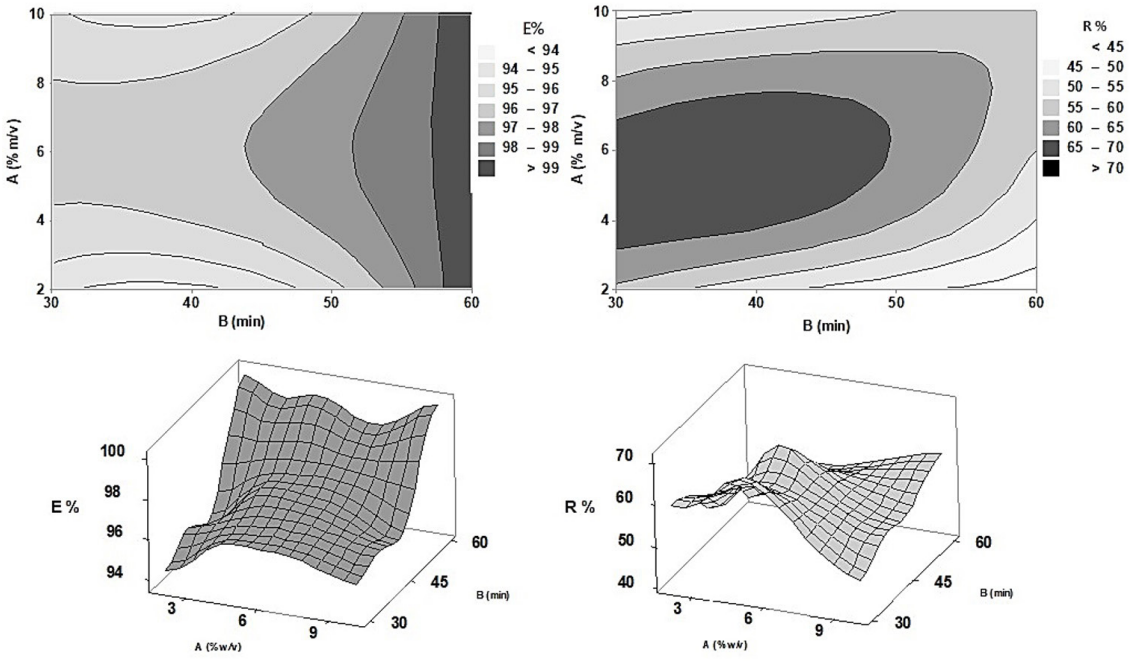

Fig. 2: The plot of (a) outline of Efficiency (E%), (b) outline of Yield (R%), (c) response surface for Efficiency (E%) and (d) response surface for Yield (R%) affected by calcium chloride concentration (A) and crosslinking time (B)

Revista Tecnología y Ciencia
DOI:https://doi.org/10.33414/rtyc.39.41-61.2020 - ISSN 1666-6933

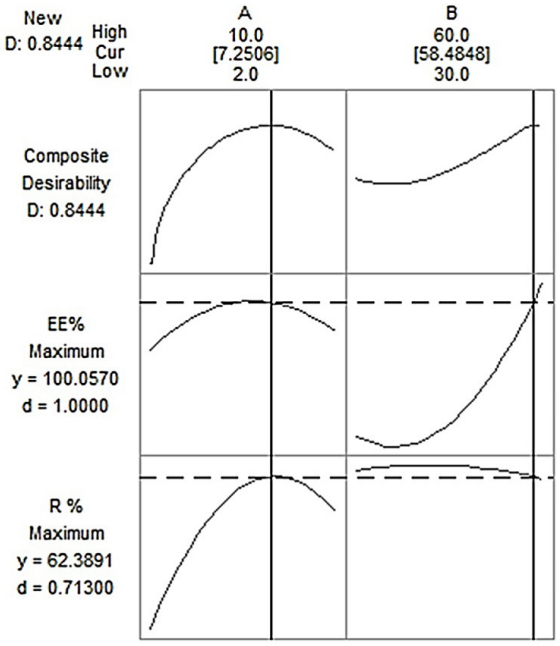

Fig. 3: The optimization plot showing the effect of the calcium chloride concentration (A) and crosslinking time (B) on the efficiency (EE%) and yield (R%).

The validation of the model was made with five runs at the optimum point, crosslinking with a calcium chloride solution of 7.4% w/v for 58 minutes. The results obtained fitted to the model, with an average efficiency of 99.97±0.02% and an average yield of 61.5±1.5%.

Loss of water in the crosslinking process

The moisture analysis was performed in quintuplicate, with a weight around 0.8 g of microcapsules (without grapefruit oil, Cl2Ca solution of 7.4% w/v, crosslinking time of 58 minutes). The average percentage moisture of microcapsules was 79.5% ±1.7% and, compared to the 99% w/w initial amount of water in the emulsion, the average water loss was 19.4% w/w. These results might be one of the reasons behind the low yield in the obtention of microcapsules.

Morphology

The microcapsules obtained by the optimized process were observed using an optical microscope equipped with a digital camera. The diameters of 50 microcapsules were measured using a data acquisition system. The average value of the measured diameter was 1.95 mm ± 0.02 mm. Figure 4a shows the optical images of the microcapsule, its spherical shape and the swollen areas due to the essential oil.

Figures 4b–d represent SEM images with different magnifications showing the porous surface of the microcapsule and a considerable number of lumps due to the presence of oil. It can also be seen the porous surface like a sponge, indicating the sodium alginate crosslinking. Similar results were obtained by Soliman et al. (2013) in the encapsulation of clove and thyme essential oil.

Revista Tecnología y Ciencia
DOI:https://doi.org/10.33414/rtyc.39.41-61.2020 ISSN 1666-6933

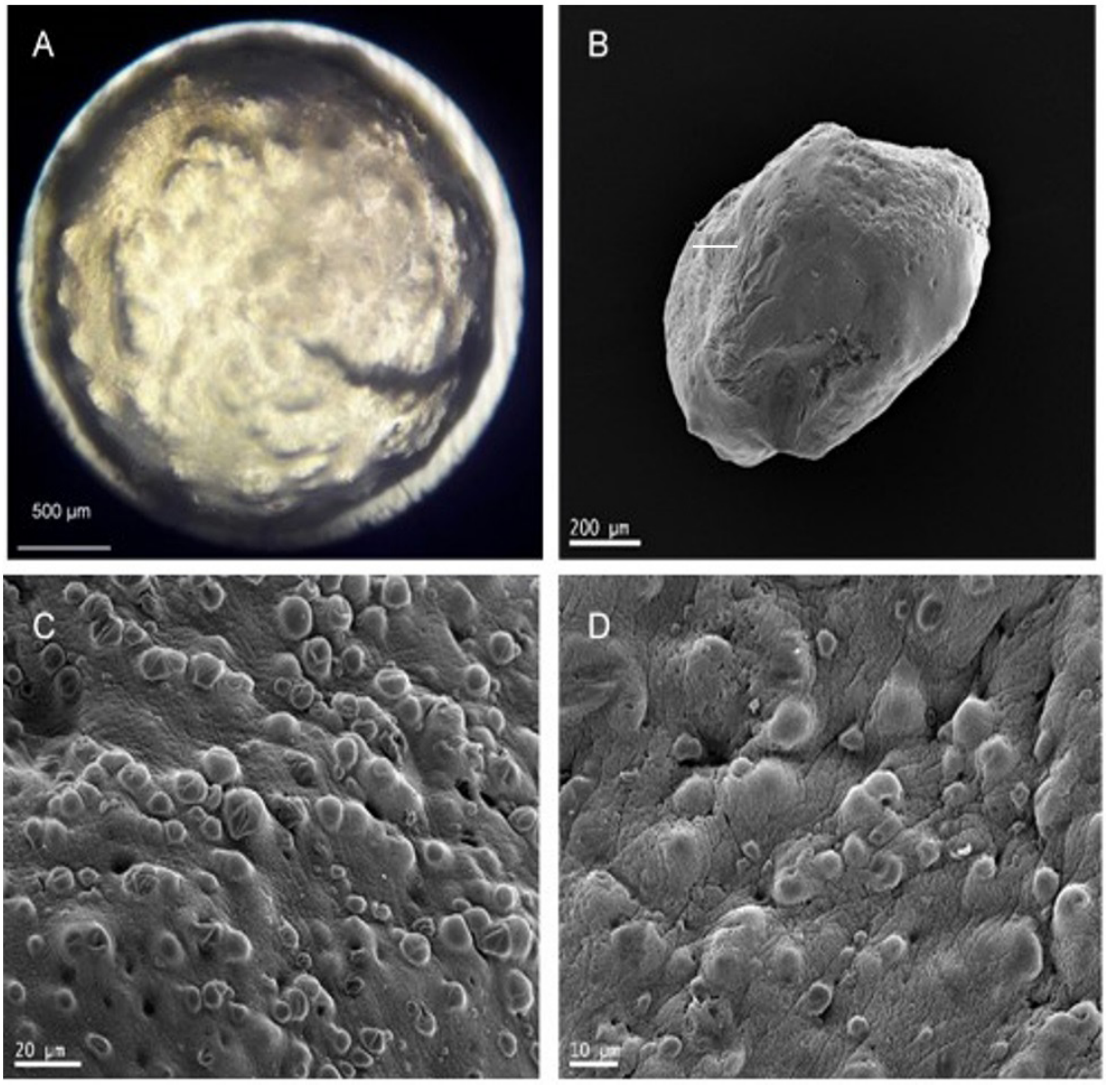

Fig. 4: Micrographs of the optimized microcapsule (with 1% (w/v) sodium alginate, 10% (w/w) grapefruit oil, 7.5% (w/v) $CaCl_2$ and 58 min of crosslinking), (a) Optical image and, (b), (c) and (d) SEM (75x, 700x and 1000x magnification respectively)

Calcium adsorption in crosslinking

The crosslinking speed was studied in a calcium chloride solution of 7.5% p/v. The average values of adsorption of calcium ions in different crosslinking times are shown in Figure 5. The adsorption speed curve followed an exponential trend and reached equilibrium at 15 minutes of crosslinking. It was assessed the empirical data fitted to the Elovich model, generally used to model the kinetics of chemisorption of solutes in the liquid phase over solids. Then, an R2 of 0.997 was obtained, which indicated a very good fitting as it is shown in Figure 5. Then, the coefficients for the integrated form of the Elovich equation were calculated as follows (9):

Revista Tecnología y Ciencia
DOI:https://doi.org/10.33414/rtyc.39.41-61.2020 - ISSN 1666-6933

$$q_t = \frac{1}{4.66}\ln(22.77 * 4.66 * t) \quad (9)$$

The value of the initial adsorption speed was 22.77 g·mg^{-1}·min^{-1}. The value of the adsorption constant (related to the square surface and the activation energy for chemisorption) was 4.66 g·mg^{-1}. While no studies were found that showed the kinetics of calcium adsorption in the crosslinking process, other works considered the adsorption speed of other metals over solid organic surfaces that fitted the Elovich model as well (Pinzón Bedoya and Vera Villamizar, 2009; Pérez-Marín et al., 2007). This model describes the chemisorption processes and supposes that the active sites of sodium alginate are heterogeneous with different activation energies (Ozacar and Şengil, 2005; Cheung et al., 2001). Figure 5 shows fast chemisorption at the beginning due to the formation of dimers that create the egg-box structure of the calcium alginate; but after five minutes, it slowed down considerably. This was explained by a progressive and uniform introduction of calcium ions caused by an increase of the surface crosslinking and continuing stirring (Teng and Hsieh, 1999). At the same time, the aggregation of the dimers led to the formation of an organized three-dimensional structure of bonds without heterogeneous grouping (Farrés and Norton, 2014).

This could also explain the influence of the crosslinking time in the efficiency of the encapsulation process. Longer crosslinking times would lead to a crosslinking network of greater order and degree of the three-dimensional "egg-box" packing, maximizing the oil transfer to the surface of the microcapsule.

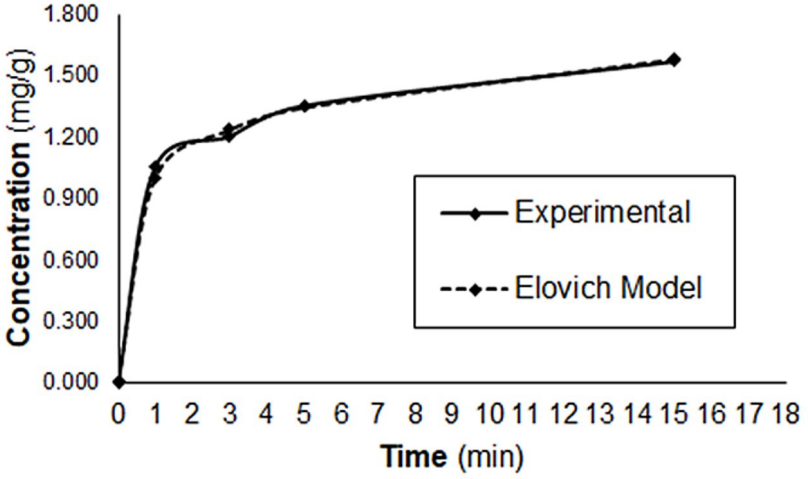

Fig. 5: Fitting of experimental calcium adsorption data to the Elovich model

Controlled Release

The controlled release study was performed with the microcapsules obtained at optimum conditions. The release of the essential oil microencapsulated in the alginate matrix was made on alcohol in order to ease its solubility. The samples taken at different times were analyzed by gas chromatography. Figure 6 shows the release compound percentage based

Revista Tecnología y Ciencia
DOI:https://doi.org/10.33414/rtyc.39.41-61.2020 ISSN 1666-6933

on time for the microcapsules prepared. The release profile had two phases: a faster one at the start, or initial "burst", and a lower one at the end (Siepmann et al., 2002). The first phase of the release could be attributed to a purely diffusional stage as a consequence of the volume expansion of the polymer due to the relaxation of its chains when submerged in liquids (Beirão-da-Costa, 2013; Hosseini et al., 2013). The almost zero-order release given below could be explained by a decrease in the release speed of the retained oil and the dispersion in the volume of the microcapsule (Hosseini et al., 2013) due to a greater distance to the surface of the microcapsule (Siepman et al., 2002). Other authors obtained similar release profiles: with eucalyptus essential oil (Noppakundilograt et al., 2015) and with oregano essential oil (Ferrándiz García, 2015). The release rate grew at 83% in 270 minutes, being faster than the rate informed by Hosseini et al. (2013) from 60 to 78% in nine hours, with 1 to 3% v/v of the loading capacity of oil. This could stem from a greater oil loading capacity in the microcapsule, which would indicate a diffusion of larger quantities of oil molecules per pore (Banerjee et al., 2012). The total release of the microencapsulated oil (90 to 100%) was obtained between 200–360 hours of sustained release, but this was not illustrated in the graphics due to the scale used. This slower release by the end could be related to the size of the particle, as bigger particles had lower release rates due to the area-volume relation (Hosseini et al., 2013). The controlled release data obtained were fitted to the Korsmeyer and Peppas semi-empirical kinetic model (1981) and the kinetic parameters of the equation (10) were obtained through a statistical analysis using the method of least squares at a 95% confidence level:

$$\frac{M_t}{M_\infty} = 2.08t^{0.475} \tag{10}$$

The value obtained of the coefficient of determination R^2 was 0.991. The value of the diffusional exponent (n) showed an anomalous (no Fickian) transport release process from a sphere (Ritger and Peppas, 1987). This result suggested that the release process was controlled by the diffusion-relaxation processes of the polymer chains, according to the results from other authors (Noppakundilograt et al., 2015; Ráquira and Yadira, 2014; Escobar et al., 2002).

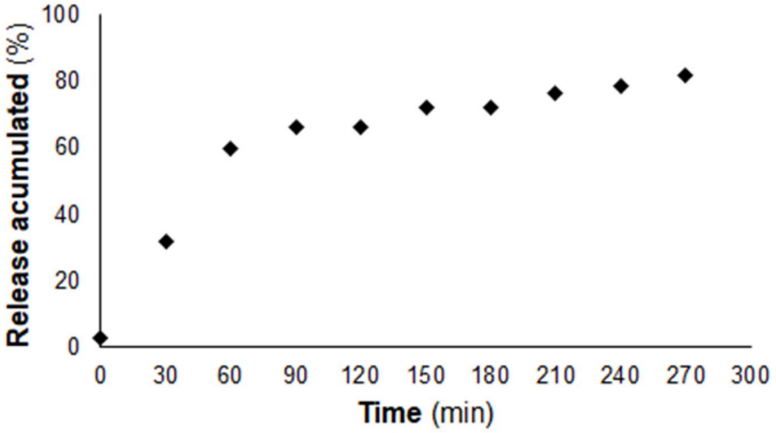

Fig. 6: Controlled release of grapefruit essential oil: at 25 °C from the microcapsules prepared with 1% (w/v) sodium alginate and 10% (w/w) grapefruit essential oil with 7.5% (w/v) CaCl2 for 58 min crosslinking time.

Revista Tecnología y Ciencia
DOI:https://doi.org/10.33414/rtyc.39.41-61.2020 - ISSN 1666-6933

Conclusion

The microencapsulation of essential grapefruit oil with sodium alginate, by external ionic gelation and extrusion, was optimized with a loading capacity of oil of 10% w/w. The validation of the optimum process, tested with the desirability function, resulted in average efficiency of 99.97±0.02% and an average yield of 61.5±1.5%. In addition, it was possible to achieve an effective controlled release in time of the essential oil encapsulated. These results positively encourage the possible use of microencapsulated grapefruit essential oil in the food industry for the conservation of certain types of dry foods.

Acknowledgments

The authors thank the company Mager SRL from the province of Corrientes, Argentina, for providing the essential grapefruit oil used in this study; the Institute IBONNE-CONNICET at Universidad Nacional del Nordeste for providing the SEM images; and the National Institute of Industrial Technology (INTI) for the analysis by atomic emission spectroscopy. The authors acknowledge financial support from Universidad Tecnológica Nacional for this research work.

Revista Tecnología y Ciencia
DOI:https://doi.org/10.33414/rtyc.39.41-61.2020 ISSN 1666-6933

References

Adams, R. P. (2007). Identification of essential oil components by gas chromatography/ mass spectrometry (Vol. 456). Carol Stream, IL: Allured publishing corporation.

Aghbashlo, M., Mobli, H., Rafiee, S., & Madadlou, A. (2012). Optimization of emulsification procedure for mutual maximizing the encapsulation and exergy efficiencies of fish oil microencapsulation, Powder technology, 225, 107-117. https://doi.org/10.1016/j.powtec.2012.03.040

Aguiar, J., Estevinho, B. N., & Santos, L. (2016). Microencapsulation of natural antioxidants for food application–The specific case of coffee antioxidants–A review, Trends in Food Science and Technology, 58, 21-39. https://doi.org/10.1016/j.tifs.2016.10.012

Arriola, N. D. A., Chater, P. I., Wilcox, M., Lucini, L., Rocchetti, G., Dalmina, M., Pearson, J. P., & Amboni, R. D. D. M. C. (2019). Encapsulation of stevia rebaudiana Bertoni aqueous crude extracts by ionic gelation–Effects of alginate blends and gelling solutions on the polyphenolic profile, Food Chemistry, 275, 123-134. https://doi.org/10.1016/j.foodchem.2018.09.086

Baranauskienė, R., Venskutonis, P. R., Dewettinck, K., & Verhé, R. (2006). Properties of oregano (Origanum vulgare L.), citronella (Cymbopogon nardus G.) and marjoram (Majorana hortensis L.) flavors encapsulated into milk protein-based matrices, Food Research International, 39(4), 413-425. https://doi.org/10.1016/j.foodres.2005.09.005

Bakkali, F., Averbeck, S., Averbeck, D., & Idaomar, M. (2008). Biological effects of essential oils–a review. Food and chemical toxicology, 46(2), 446-475. https://doi.org/10.1016/j.fct.2007.09.106

Bal, T., Sengupta, S., & Murthy, P. N. (2013). Formulation and evaluation of carvedilol microcapsules using Eudragit NE30D and sodium alginate, Brazilian journal of pharmaceutical sciences, 49(4), 889-901. http://dx.doi.org/10.1590/S1984-82502013000400029

Balanč, B., Trifković, K., Dordević, V., Marković, S., Pjanović, R., Nedović, V., & Bugarski, B. (2016). Novel resveratrol delivery systems based on alginate-sucrose and alginate-chitosan microbeads containing liposomes, Food Hydrocolloids, 61, 832-842. http://dx.doi.org/10.1016/j.foodhyd.2016.07.005

Beirão-da-Costa, S., Duarte, C., Bourbon, A. I., Pinheiro, A. C., Januário, M. I. N., Vicente, A. A., ... & Delgadillo, I. (2013). Inulin potential for encapsulation and controlled delivery of Oregano essential oil, Food Hydrocolloids, 33(2), 199-206. http://dx.doi.org/10.1016/j.foodhyd.2013.03.009

Belscak-Cvitanovic, A., Bušić, A., Barisic, L., Vrsaljko, D., Karlovic, S., Spoljaric, I. & Komes, D. (2016). Emulsion templated microencapsulation of dandelion (Taraxacum officinale L.) polyphenols and β-carotene by ionotropic gelation of alginate and pectin, Food hydrocolloids, 57, 139-152. http://dx.doi.org/10.1016/j.foodhyd.2016.01.020

Banerjee, S., Chattopadhyay, P., Ghosh, A., Goyary, D., Karmakar, S., & Veer, V. (2013). Influence of process variables on essential oil microcapsule properties by carbohydrate polymer–protein blends, Carbohydrate polymers, 93(2), 691-697. https://doi.org/10.1016/j.carbpol.2013.01.028

Benavides, S., Cortés, P., Parada, J., & Franco, W. (2016). Development of alginate

Revista Tecnología y Ciencia
DOI:https://doi.org/10.33414/rtyc.39.41-61.2020 - ISSN 1666-6933

microspheres containing thyme essential oil using ionic gelation, Food chemistry, 204, 77-83. http://dx.doi.org/10.1016/j.foodchem.2016.02.104

Camino, N. A., Sanchez, C. C., Patino, J. M. R., & Pilosof, A. M. (2012). Hydroxypropylmethylcellulose–β-lactoglobulin mixtures at the oil–water interface. Bulk, interfacial and emulsification behavior as affected by pH, Food Hydrocolloids, 27(2), 464-474. https://doi.org/10.1016/j.foodhyd.2011.09.006

Chan, L. W., Lim, L. T., & Heng, P. W. S. (2000). Microencapsulation of oils using sodium alginate, Journal of microencapsulation, 17(6), 757-766. https://doi.org/10.1080/02652040050161747

Chan, E. S. (2011). Preparation of Ca-alginate beads containing high oil content: Influence of process variables on encapsulation efficiency & bead properties, Carbohydrate polymers, 84(4), 1267-1275. https://doi.org/10.1016/j.carbpol.2011.01.015

Chen, F., Liang, L., Zhang, Z., Deng, Z., Decker, E. A., & McClements, D. J. (2017). Inhibition of lipid oxidation in nanoemulsions and filled microgels fortified with omega-3 fatty acids using casein as a natural antioxidant, Food Hydrocolloids, 63, 240-248. https://doi.org/10.1016/j.foodhyd.2016.09.001

Cheung, C. W., Porter, J. F., & McKay, G. (2001). Sorption kinetic analysis for the removal of cadmium ions from effluents using bone char, Water Research, 35(3), 605-612. https://doi.org/10.1016/S0043-1354(00)00306-7

Chuah, A. M., Kuroiwa, T., Kobayashi, I., Zhang, X. & Nakajima, M. (2009). Preparation of uniformly sized alginate microspheres using the novel combined methods of microchannel emulsification and external gelation, Colloids and Surfaces A: Physicochemical and Engineering Aspects, 351(1-3), 9-17. https://doi.org/10.1016/j.colsurfa.2009.09.005

Dima, C., Cotârlet, M., Alexe, P., & Dima, S. (2014). Microencapsulation of essential oil of pimento [Pimenta dioica (L) Merr.] by chitosan/k-carrageenan complex coacervation method, Innovative Food Science and Emerging Technologies, 22, 203-211. https://doi.org/10.1016/j.ifset.2013.12.020

Ding, W. K. & Shah, N. P. (2007). Acid, bile, and heat tolerance of free and microencapsulated probiotic bacteria, Journal of food science, 72(9), M446-M450. https://doi.org/10.1111/j.1750-3841.2007.00565.x

Escobar, J. L., García, D. M., Zaldivar, D., & Katime, I. (2002). Hidrogeles. Principales características en el diseño de sistemas de liberación controlada de fármacos, Revista Iberoamericana, 3(3). Retrieved on April 9, 2019, from http://www.ehu.eus/reviberpol/pdf/Jul/escobar2.pdf

Goitia Funes, M. B., & Amurrio Derpic, D. (2016). Micro-encapsulación de aceite de chía, Acta Nova, 7(3), 289-302. Retrieved on April 13, 2019, from http://www.scielo.org.bo/scielo.php?script=sci_arttext&pid=S1683-07892016000100006&lng=es&tlng=es

Goh, C. H., Heng, P. W. S., & Chan, L. W. (2012). Alginates as a useful natural polymer for microencapsulation and therapeutic applications, Carbohydrate Polymers, 88(1), 1-12. https://doi.org/10.1016/j.carbpol.2011.11.012

González, N., Fernández, D., Gómez, M., Núñez, L., & Lafita, O. (2005). Efecto del Eudragit

Revista Tecnología y Ciencia
DOI:https://doi.org/10.33414/rtyc.39.41-61.2020 ISSN 1666-6933

y la Etilcelulosa como agentes retardantes de la liberación sobre las características físico-químicas y la liberación in vitro de microesferas cargadas con zidovudina, Acta Farmaceutica Bonaerense, 24(3), 350-355. Retrieved on April 7, 2019 from http://www.latamjpharm.org/trabajos/24/3/LAJOP_24_3_1_5_9GQ241739C.pdf

Faisant, N., Siepmann, J., Richard, J., & Benoit, J. P. (2003). Mathematical modeling of drug release from bioerodible microparticles: effect of gamma-irradiation, European Journal of Pharmaceutics and Biopharmaceutics, 56(2), 271-279. doi:10.1016/S0939-6411(03)00104-8

Farrés, I. F., & Norton, I. T. (2014). Formation kinetics and rheology of alginate fluid gels produced by in-situ calcium release, Food Hydrocolloids, 40, 76-84. http://dx.doi.org/10.1016/j.foodhyd.2014.02.005

Federcitrus. (2018). The Argentine Citrus Industry. Retrieved from https://www.federcitrus.org/wp-content/uploads/2018/05/Actividad-Citricola-2018.pdf

Ferrándiz García, M. (2015). Encapsulación de aceites esenciales funcionales para su aplicación en agricultura [unpublished doctoral thesis]. Polytechnic University of Valencia. http://hdl.handle.net/10251/58990

Finch, C. A. (2005). Encapsulation and controlled release. (D.R. Karsa and R.A. Stephenson, eds.). Cambridge: Woodhead Publishing limited, 1-12. Retrieved on April 7, 2019, from https://epdf.tips/encapsulation-and-controlled-release-woodhead-publishing-series-in-food-science-.html

Hosseini, S. M., Hosseini, H., Mohammadifar, M. A., Mortazavian, A. M., Mohammadi, A., Khosravi-Darani, K., Shojaee-Aliabadi, S., Dehghanc, S., & Khaksar, R. (2013). Incorporation of essential oil in alginate microparticles by multiple emulsion/ionic gelation process, International journal of biological macromolecules, 62, 582-588. https://doi.org/10.1016/j.ijbiomac.2013.09.054

Jun-xia, X., Hai-yan, Y., & Jian, Y. (2011). Microencapsulation of sweet orange oil by complex coacervation with soybean protein isolate/gum Arabic, Food Chemistry, 125(4), 1267-1272. https://doi.org/10.1016/j.foodchem.2010.10.063

Korsmeyer, R. W., & Peppas, N. A. (1981). Effect of the morphology of hydrophilic polymeric matrices on the diffusion and release of water-soluble drugs, Journal of Membrane Science, 9(3), 211-227. https://doi.org/10.1016/S0376-7388(00)80265-3

Kuang, S. S., Oliveira, J. C., & Crean, A. M. (2010). Microencapsulation as a tool for incorporating bioactive ingredients into food, Critical Reviews in Food Science and Nutrition, 50(10), 951-968. https://doi.org/10.1080/10408390903044222

Kuehl, R. O., & Kuehl, R. O. (2000). Design of experiments: statistical principles of research design and analysis (2.ª ed.). Thomson Learning. México, 175-225.

Laokuldilok, N., Thakeow, P., Kopermsub, P., & Utama-Ang, N. (2016). Optimisation of microencapsulation of turmeric extract for masking flavour, Food chemistry, 194, 695-704. https://doi.org/10.1016/j.foodchem.2015.07.150

Lević, S., Lijaković, I. P., Dordević, V., Rac, V., Rakić, V., Knudsen, T. S., Pavlović, V., Bugarski, B. & Nedović, V. (2015). Characterization of sodium alginate/d-limonene emulsions and respective calcium alginate/d-limonene beads produced by electrostatic extrusion, Food Hydrocolloids, 45, 111-123. https://doi.org/10.1016/j.foodhyd.2014.10.001

Revista Tecnología y Ciencia
DOI:https://doi.org/10.33414/rtyc.39.41-61.2020 - ISSN 1666-6933

Lertsutthiwong, P., Noomun, K., Jongaroonngamsang, N., Rojsitthisak, P., & Nimmannit, U. (2008). Preparation of alginate nanocapsules containing turmeric oil, Carbohydrate polymers, 74(2), 209-214. https://doi.org/10.1016/j.carbpol.2008.02.009

Liakos, I., Rizzello, L., Scurr, D. J., Pompa, P. P., Bayer, I. S., & Athanassiou, A. (2014). All-natural composite wound dressing films of essential oils encapsulated in sodium alginate with antimicrobial properties, International journal of pharmaceutics, 463(2), 137-145. https://doi.org/10.1016/j.ijpharm.2013.10.046

Liu, K., Xu, Y., & Wang, X. (2012). Microencapsulation of sweet orange oil terpeneless using the orifice method, Journal of food engineering, 110(3), 390-394. https://doi.org/10.1016/j.jfoodeng.2011.12.033

Lupo, B., Maestro, A., Gutiérrez, J. M., & González, C. (2015). Characterization of alginate beads with encapsula ted cocoa extract to prepare functional food: comparison of two gelation mechanisms, Food Hydrocolloids, 49, 25-34. https://doi.org/10.1016/j.foodhyd.2015.02.023

Lv, Y. X., Zhao, S. P., Zhang, J. Y., Zhang, H., Xie, Z. H., Cai, G. M., & Jiang, W. H. (2012). Effect of orange peel essential oil on oxidative stress in AOM animals, International journal of biological macromolecules, 50(4), 1144-1150. https://doi.org/10.1016/j.ijbiomac.2012.02.002

Mabille, C., Schmitt, V., Gorria, P., Leal Calderon, F., Faye, V., Deminiere, B., & Bibette, J. (2000). Rheological and shearing conditions for the preparation of monodisperse emulsions, Langmuir, 16(2), 422-429. https://pubs.acs.org/doi/pdf/10.1021/la990850w

Maji, T. K., Baruah, I., Dube, S., & Hussain, M. R. (2007). Microencapsulation of Zanthoxylum limonella oil (ZLO) in glutaraldehyde crosslinked gelatin for mosquito repellent application, Bioresource Technology, 98(4), 840-844. https://doi.org/10.1016/j.biortech.2006.03.005

McLafferty, F. W., & Stauffer, D. B. (2009). Wiley registry of mass spectral data (Vol. 662). Hoboken, NJ: John Wiley.Wiley, New York.

Mokhtari, S., Jafari, S. M., & Assadpour, E. (2017). Development of a nutraceutical nano-delivery system through emulsification/internal gelation of alginate, Food chemistry, 229, 286-295. https://doi.org/10.1016/j.foodchem.2017.02.071

Montgomery, D. C. (2003). Diseño y análisis de experimentos, Ed. Limusa Wiley, México.

Noppakundilograt, S., Piboon, P., Graisuwan, W., Nuisin, R., & Kiatkamjornwong, S. (2015). Encapsulated eucalyptus oil in ionically cross-linked alginate microcapsules and its controlled release, Carbohydrate polymers, 131, 23-33. https://doi.org/10.1016/j.carbpol.2015.05.054

Özacar, M., & Şengil, İ. A. (2005). A kinetic study of metal complex dye sorption onto pine sawdust, Process Biochemistry, 40(2), 565-572. https://doi.org/10.1016/j.procbio.2004.01.032

Pérez-Marín, A. B., Zapata, V. M., Ortuno, J. F., Aguilar, M., Sáez, J., & Lloréns, M. (2007). Removal of cadmium from aqueous solutions by adsorption onto orange waste, Journal of hazardous materials, 139(1), 122-131. https://doi.org/10.1016/j.jhazmat.2006.06.008

Pinzón-Bedoya, M. L., & Vera Villamizar, L. E. (2009). Kinetc modeling biosorption of Cr (III) using orange shell, Dyna, 76(160), 95-106.

Revista Tecnología y Ciencia
DOI:https://doi.org/10.33414/rtyc.39.41-61.2020 ISSN 1666-6933

Ráquira, A., & Yadira, Í. Preparación y evaluación en suelo de fertilizantes de liberación controlada cubiertos con polímeros biodegradables. [unpublished doctoral thesis], Universidad Nacional de Colombia. Retrieved from https://core.ac.uk/download/pdf/77267086.pdf

Ribeiro, A. J., Neufeld, R. J., Arnaud, P., & Chaumeil, J. C. (1999). Microencapsulation of lipophilic drugs in chitosan-coated alginate microspheres, International journal of pharmaceutics, 187(1), 115-123. https://doi.org/10.1016/S0378-5173(99)00173-8

Ribeiro-Santos, R., Andrade, M., & Sanches-Silva, A. (2017). Application of encapsulated essential oils as antimicrobial agents in food packaging, Current Opinion in Food Science, 14, 78-84. https://doi.org/10.1016/j.cofs.2017.01.012

Ritger, P. L., & Peppas, N. A. (1987). A simple equation for description of solute release I. Fickian and non-fickian release from non-swellable devices in the form of slabs, spheres, cylinders or discs, Journal of controlled release, 5(1), 23-36. https://doi.org/10.1016/0168-3659(87)90034-4

Shori, A. B. (2017). Microencapsulation improved probiotics survival during gastric transit, Journal of Biosciences, 24(1), 1-5. https://doi.org/10.1016/j.hjb.2016.12.008

Siepmann, J., Faisant, N., & Benoit, J. P. (2002). A new mathematical model quantifying drug release from bioerodible microparticles using Monte Carlo simulations, Pharmaceutical research, 19(12), 1885-1893. https://doi.org/10.1023/A:1021457911533

Sis, H., Kelbaliyev, G., & Chander, S. (2005). Kinetics of drop breakage in stirred vessels under turbulent conditions, Journal of dispersion science and technology, 26(5), 565-573. https://doi.org/10.1081/DIS-200057638

Soliman, E. A., El-Moghazy, A. Y., El-Din, M. M., & Massoud, M. A. (2013). Microencapsulation of essential oils within alginate: formulation and in vitro evaluation of antifungal activity, Journal of Encapsulation and Adsorption Sciences, 3(01), 48. http://dx.doi.org/10.4236/jeas.2013.31006 P

Solomon, B., Sahle, F. F., Gebre-Mariam, T., Asres, K., & Neubert, R. H. H. (2012). Microencapsulation of citronella oil for mosquito-repellent application: formulation and in vitro permeation studies, European Journal of Pharmaceutics and Biopharmaceutics, 80(1), 61-66. https://doi.org/10.1016/j.ejpb.2011.08.003

Teng, H., & Hsieh, CT (1999). Energía de activación para la quimiosorción de oxígeno sobre carbono a bajas temperaturas, Investigación en química industrial y de ingeniería, 38 (1), 292-297. https://doi: 10.1021 / ie980107j

Tuyen, C. K., Nguyen, M. H., Roach, P. D., & Stathopoulos, C. E. (2014). Microencapsulation of gac oil: optimisation of spray drying conditions using response surface methodology, Powder Technology, 264, 298-309. https://doi.org/10.1016/j.powtec.2014.05.053

Vasek, O. M., Cáceres, L. M., Chamorro, E. R., & Velasco, G. A. (2015). Antibacterial activity of Citrus paradisi essential oil, Journal of Natural Products, 8, 16-26. Retrieved on 5 April, 2019, from http://ria.utn.edu.ar/bitstream/handle/123456789/941/AntibacterialActivity_vf.pdf?sequence=1&isAllowed=y